Charact ristics of τ-Form Metal-Fr Phthalocyanine and Its Improvement for Organic Photoreceptor Use

T shio Enokida

Graduate School of Science and Technology, Chiba University, 1-33 Yayoi-cho, Chiba-shi 260, Japan

Ry Hirohashi

Faculty of Engineering, Chiba University, 1-33 Yayoi-cho, Chiba-shi 260, Japan

Satoshi Mizukami

Electronic Materials Division, Toyo Ink Mfg. Co., Ltd., 1 Sakae, Kawagoe-shi 350, Japan

Effects of particle shape on τ-form metal-free phthalocyanine (τ-H_2Pc) for charge generation material were investigated. Continuing the milling for preparation of particles, we could change the particle shape of τ-H_2Pc from needle-like (Type I) to granular (Type II) in a crystal conversion process. Differences of the analytical, electrical, and electrophotographic properties can be seen between Type I and Type II. The photoreceptor of Type II exhibited excellent electrophotographic properties relative to those of Type I. In particular, the half-decay exposure ($E_{1/2}$) of a dual-layered photoreceptor of Type II for charge generation material and butadiene derivative for charge transport material measured 2.5 ergs/cm^2 at 780 nm.

Journal of Imaging Science 35: 235 – 239 (1991)

Introduction

Compact laser beam printers (LBP) equipped with GaAlAs laser diodes, which emit wavelengths longer than approximately 750 nm, have been placed on the market. Photoreceptors with a photoresponse in the near-infrared region of 760–830 nm are therefore needed for LBP applications. For this reason, active research is under way with regard to dual-layered photoreceptors using organic materials, such as phthalocyanines, for charge generation materials (CGM).

It has been reported that photosensitivity depends on the crystal form of phthalocyanines.[1] We have been investigating dual-layered organic photoreceptors incorporating τ-form metal-free phthalocyanine (τ-H_2Pc) as CGM.[2,3] In general, H_2Pc has low sensitivity in the near-infrared; however, the τ-H_2Pc showed excellent sensitivity in the near-infrared region following crystal transformation with polyethylene glycol milling. Thus, the investigation of particle shapes becomes more important for highly sensitive photoreceptors. In particular, we observed the crystal structures and electrophotographic differences of two shapes of τ-H_2Pc, the needle-like particles (Type I) and the granular particles (Type II).

In this paper we report the characteristics of τ-H_2Pc compared with other polymorphs of H_2Pc and the differences between the two shapes of τ-H_2Pc for LBP printing system use.

Experimental

Materials and Sample Preparation. The polymorphic transition processes of H_2Pc are shown in Fig. 1. Crude β-H_2Pc was synthesized by the reaction of phthalonitrile in organic inert solvent. The reaction product was purified by solvent extraction. The α-H_2Pc was prepared from crude β-H_2Pc by the acid-pasting method. The τ-H_2Pc was prepared from acid-pasted α-H_2Pc by wet milling in polyethylene glycol. The shape of the τ-H_2Pc particles was needle-like (Type I). The milling time duration was approximately 20 hr in the temperature range 60–130 °C. The new Type II was then prepared by wet milling of Type I for approximately 10 hr in the same pot. After that process, the shape of the particles had changed from needle-like to granular. The granular τ-H_2Pc was designated Type II.

The surface-type cell for electric measurements consists of two interpenetrating combs spaced 0.5 mm apart. Electrodes are made by depositing Au onto the surface of the H_2Pc. The total area of H_2Pc is 24.0 mm^2.

Structures of the materials used for CGM and the charge transport material (CTM) are shown in Fig. 2. The substrate is an aluminum plate. The charge genera-

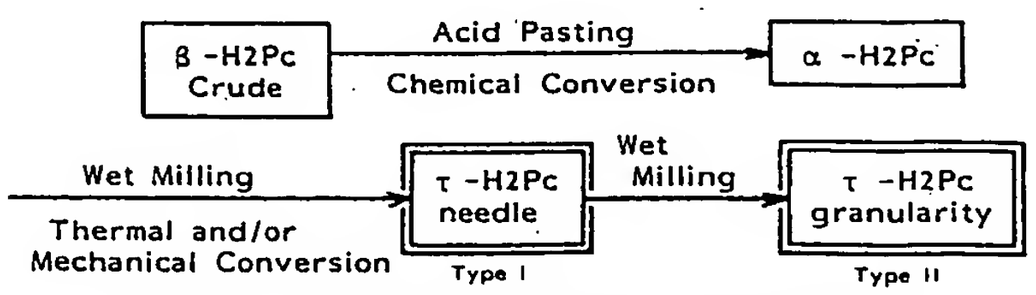

Figure 1. Polymorphic transition process of H_2Pc.

Presented at SPSE 6th International Congress on Advances in Non-Impact Printing Technologies, Oct. 21-26, 1990, Orlando, Florida.
Received Jan. 3, 1991; revised Mar. 25, 1991.

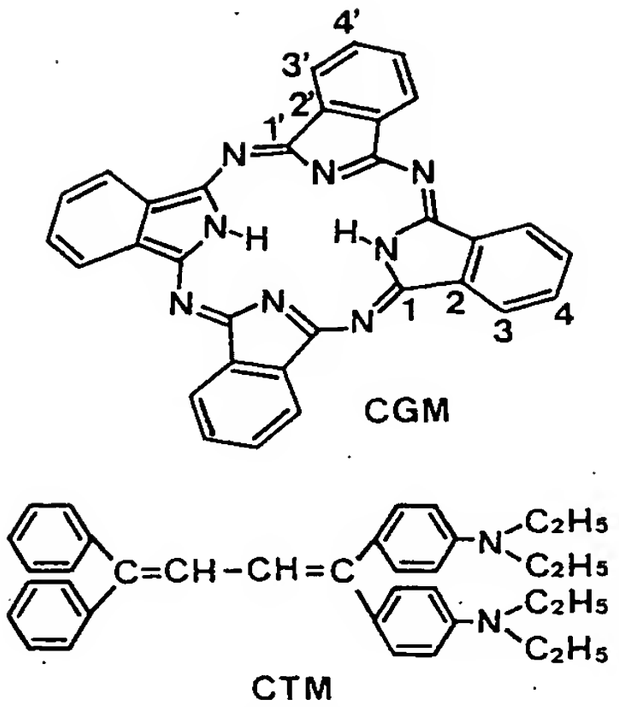

Figure 2. Structures of CGM and CTM.

tion layer (CGL) consists of 50 wt % of a CGM dispersed in poly(vinylbutyral) with thickness of 0.2 μm. The charge transport layer (CTL) is composed of 50 wt % butadiene derivative in bisphenol-A-polycarbonate on the CGL. The CTL thickness is 20 μm.

Measurements. Solid-state cross-polarization/magic angle spinning (CP/MAS) ^{13}C-NMR spectra were measured at room temperature on a JEOL GSX-270W spectrometer at the frequency of 67.5 MHz. The techniques of CP/MAS were employed to enhance signal-to-noise ratio and spectral resolution. Resolution was within 5 Hz at the spinning speed of 4.5 kHz. The ^{13}C chemical shifts were determined by using liquid tetramethyl silane (TMS) as an external reference. X-ray powder diffraction patterns were recorded on a Rigaku-Denki RU-200 diffractometer equipped with CuK α monochromatic radiation. Absorption spectra of films were recorded on a UV-2100S spectrophotometer (Japan Spectroscopic Co., Ltd.). Average particle sizes of H_2Pc were measured by a Shimadzu SA-CP3 centrifugal particle analyzer for dispersed particles in THF.

The cell current was measured by a Keithley 617 electrometer at 2×10^{-6} Torr. The cell was illuminated with a 500 W xenon lamp. Hole carrier drift mobility was measured by the usual time-of-flight (TOF) technique. A pulse of a 337-nm N_2 laser (5 nsec) was used to generate carriers in CTL through a NESA glass substrate. An opposite electrode was deposited onto the surface of CTL. Electrophotographic measurements were made with a Kawaguchi Electric EPA-8100 Electrophotographic Paper Analyzer. The wavelength was adjusted with interference filters. For determining cyclic stability, three surface potentials were measured: the potential just before exposure, V_{dark}, the potential at -200 V after exposure, V_{light}, and the residual potential after erase, V_{res}.

Results and Discussion

Solid-State CP/MAS ^{13}C-NMR Spectra. The IR spectra, absorption spectra, and x-ray diffraction data have been used to distinguish the crystal forms of phthalocyanines. We found that the solid-state CP/MAS ^{13}C-NMR spectroscopy was also a useful method to analyze the crystal state of phthalocyanines.[5,6]

Figure 3 shows the solid-state CP/MAS ^{13}C-NMR spectra of α, β, and τ-H_2Pc. It is possible to distinguish the environment-modulated proton tautomerism of H_2Pc. The proton dynamics in α-H_2Pc were observed using the two-dimensional chemical exchange in the solid-state by Meier et al.[7] The broad shifts of α-H_2Pc show a rapid N – H $\cdots$ N proton exchange velocity, and many shifts of β-H_2Pc show a slow velocity. The τ-H_2Pc has eight well-split sharp shifts because of the appropriate distance and arrangement by the interaction between neighboring H_2Pc molecules. We can identify the spectra of Type I and Type II; therefore, this spectral result shows the differences of packing state with H_2Pc molecules.

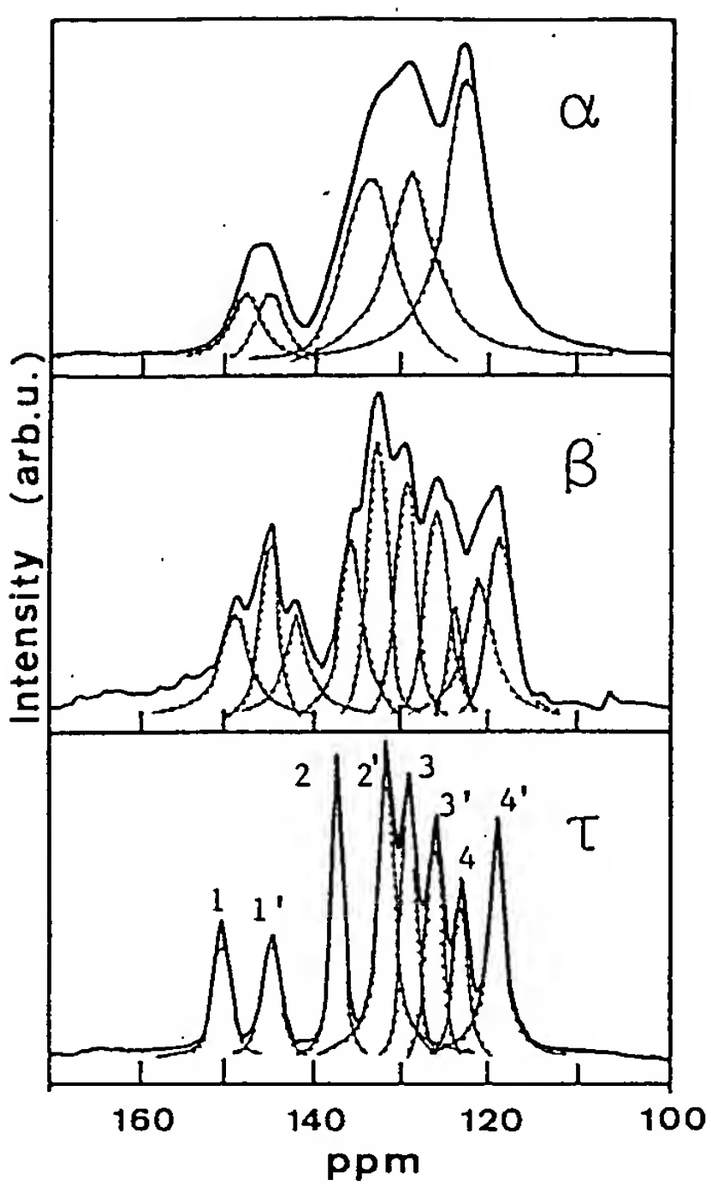

Figure 3. Solid-state CP/MAS ^{13}C-NMR spectra of H_2Pc.

Numbers were assigned to the carbons of τ-H_2Pc in Fig. 2. The differences of crystal forms in crystallographic, spectroscopic, and photoconducting properties are attributable to distinct stacking of phthalocyanine molecules and the states of inner protons.

Scanning Electron Micrographs of Particles. Figure 4 shows scanning electron micrographs (SEM) of Type I and Type II τ-H_2Pc particles. The two types of τ-H_2Pc can be distinguished. The shape of Type I particles is needle-like and that of Type II is granular. With the same process, we could produce τ-H_2Pc particles having average particle sizes over 5 μm. The usual CGL thickness in the dual-layered photoreceptor is approximately 0.5 μm; therefore, we did not use the larger particles in this study.

X-Ray Powder Diffraction Patterns. Figure 5 shows the x-ray powder diffraction patterns of Types I and II τ-H_2Pc. Both types of τ-H_2Pc exhibit strong lines at Bragg angles (2θ) of 7.6, 9.2, 16.8, 17.4, 20.4, and 20.9°. Positions of peaks were almost identical; however, the intensity of peaks below 4.15 Å was stronger in Type II

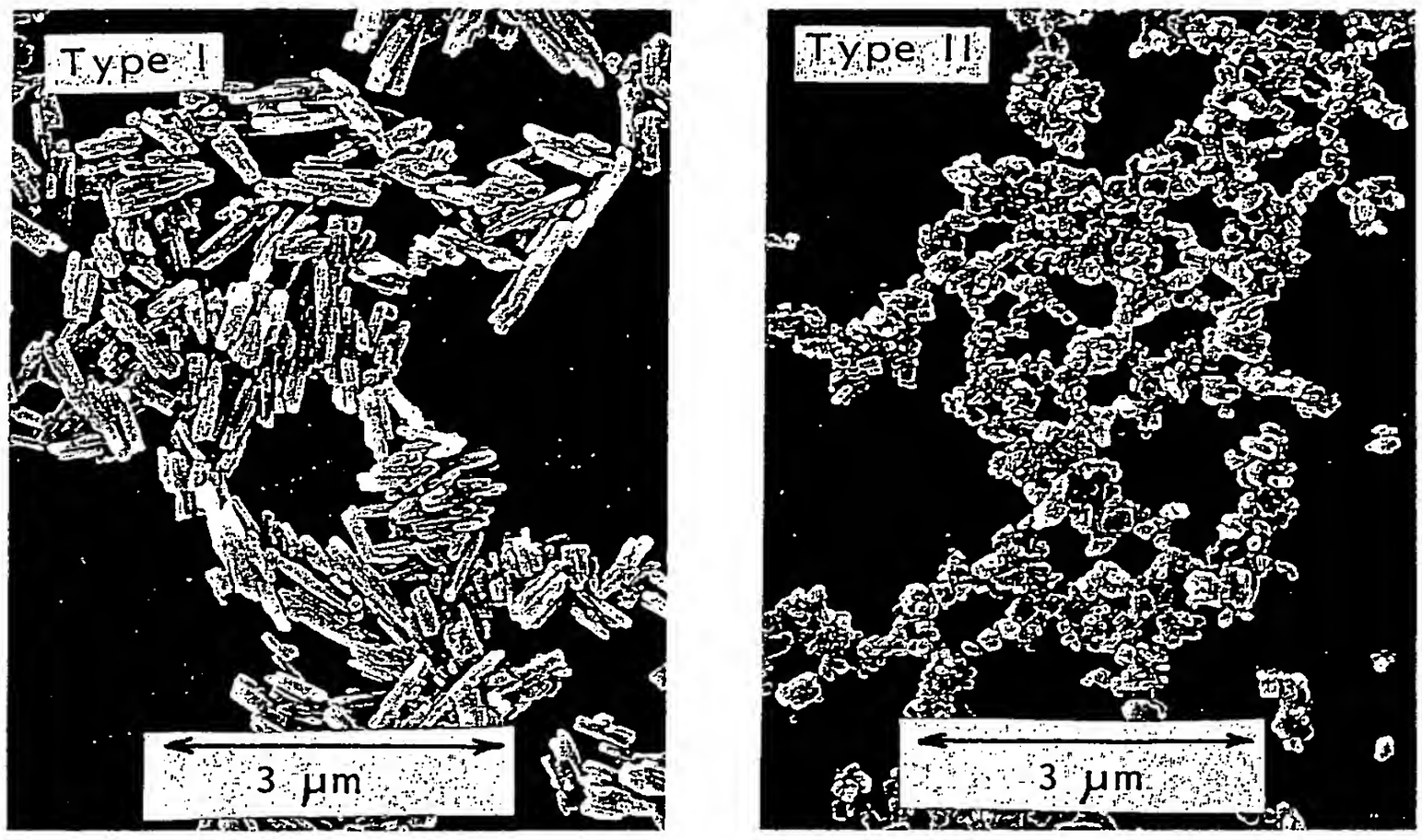

Figure 4. Scanning electron micrographs of τ-H_2Pc.

than in Type I. This is because the crystallinity of Type II is promoted in the process of additional wet milling. Other organic pigments, such as azoic and perylene compounds, also show this tendency. The strong intensities of the x-ray powder diffraction peaks over 20° means both high crystallinity of packed molecules and large surface area of particles.

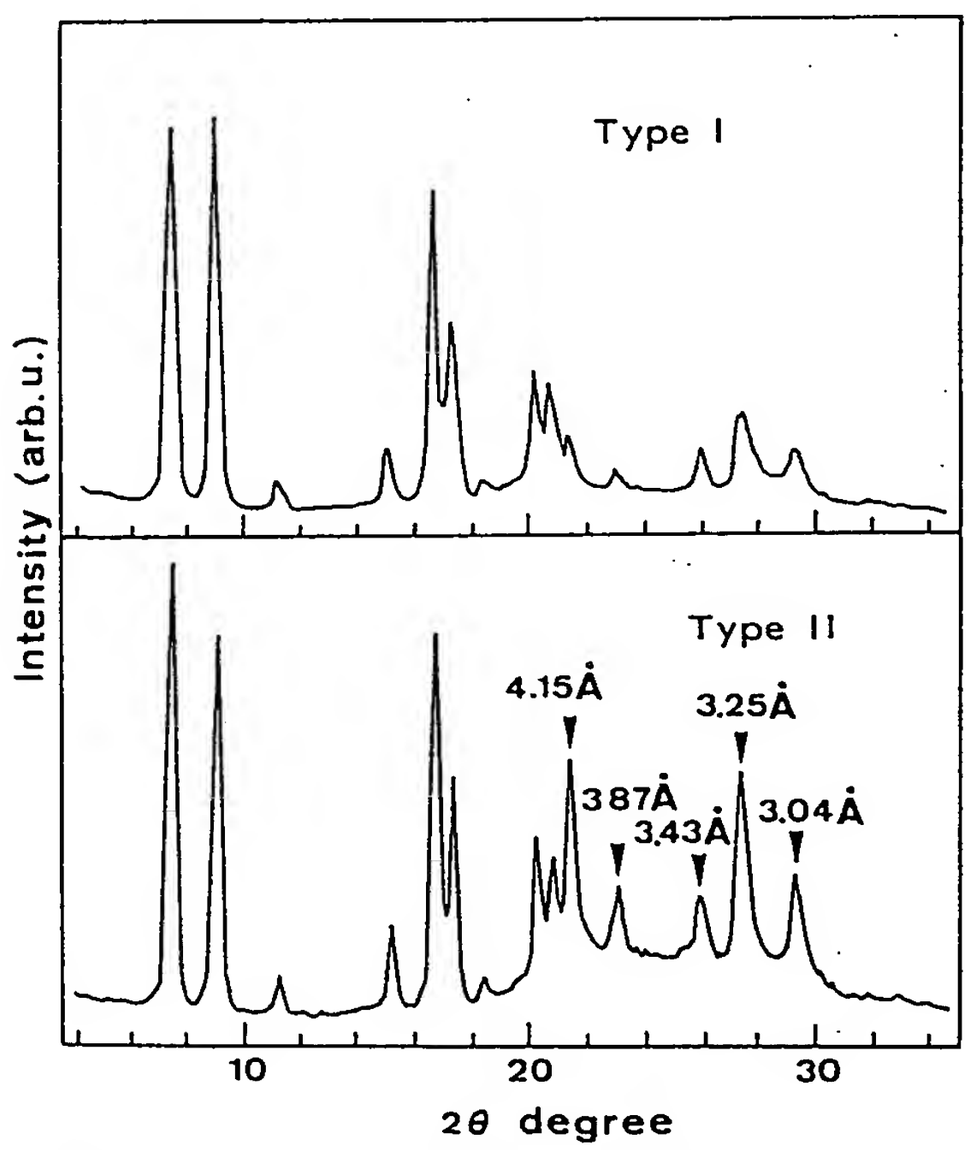

Figure 5. X-ray powder diffraction patterns of τ-H_2Pc.

Relationship of Absorption Spectra and Particle Sizes. Absorption spectra of the CGL and CTL films are shown in Fig. 6. Three absorption maxima are observed in the τ-H_2Pc film spectra. The spectra beyond 780 nm (λ_{max}) in the τ-H_2Pc films are particularly unique, and those wavelengths are suitable for GaAlAs diode lasers.

The λ_{max} wavelengths were influenced by the size of particles. The relationship of λ_{max} and average particle size, including both Type I and Type II, are shown in Fig. 7. These average particle sizes are measured by a centrifugal particle size analyzer, using particles dispersed in THF. The data follow a straight line in this region; thus λ_{max} values are easily altered by particle size change. The λ_{max} wavelength also depends on the concentration of τ-H_2Pc dispersed in THF; the λ_{max} of a more concentrated sample was shifted toward the shorter wavelength region. This phenomenon may be correlated to the state of aggregation of τ-H_2Pc in solvent and to scattering effects on the light irradiation from the spectrophotometer.

Electrical Characteristics. The H_2Pc particles contain charge carrier traps, which originate from structural irregularities and impurities. The dark conductivity and

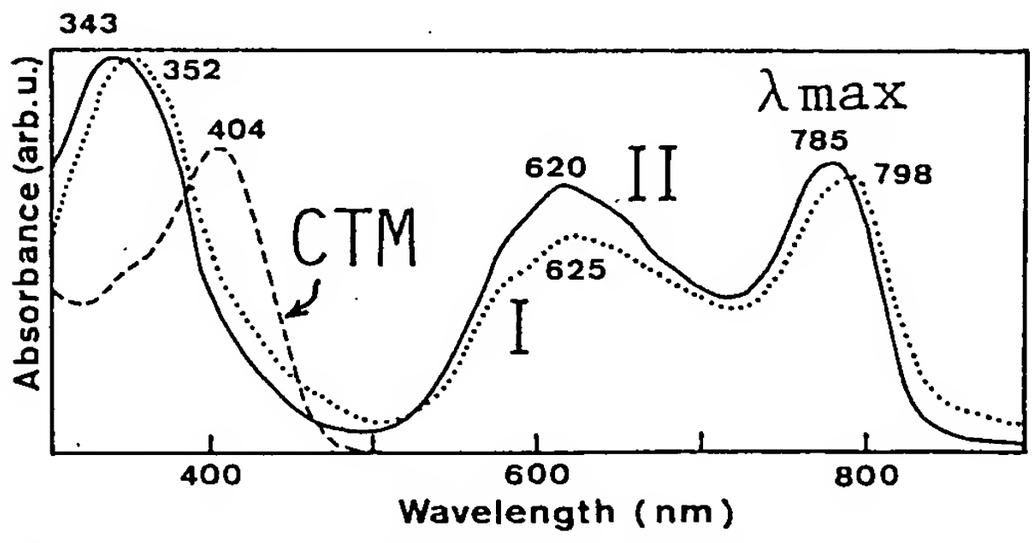

Figure 6. Absorption spectra of CGL and CTL.

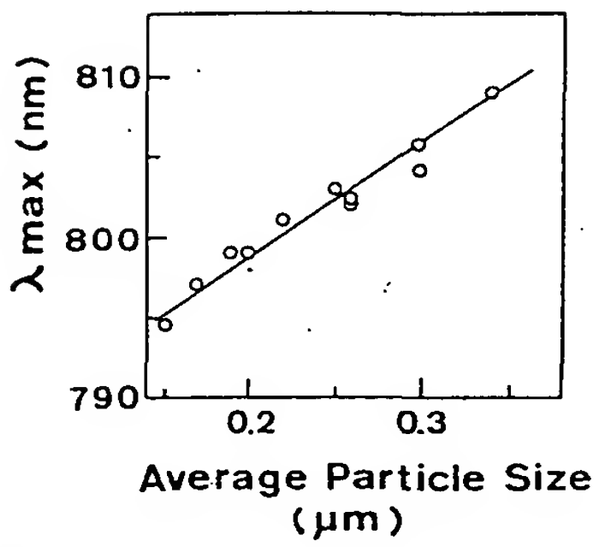

Figure 7. Relationship of λ_{max} and average particle sizes of τ-H_2Pc.

photoconductivity of H_2Pc are affected by these traps. Therefore, it is necessary to measure the dependence of electrical current on applied voltage. The dark current (Id) and photocurrent (Iph) of H_2Pc are shown in Fig. 8.

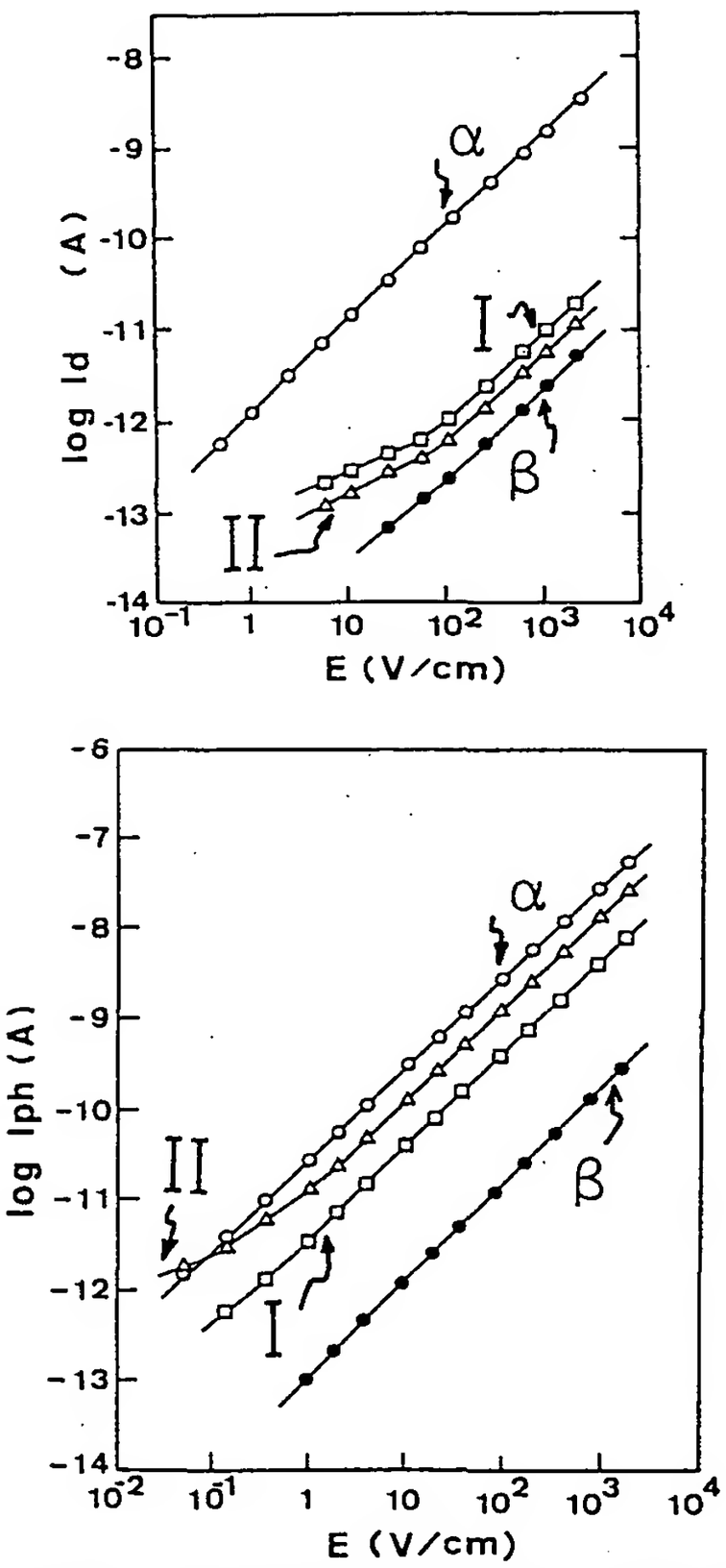

Figure 8. Dark current (Id) and photo current (Iph) of H_2Pc.

The Id and electric fields were connected via a linear relationship corresponding to Ohmic contact. The α-H_2Pc showed larger Id than the other polymorphic forms, reflecting the differences of crystal arrangement. These large Id are attributable to the fast exchange velocities of hydrogen ions in H_2Pc molecules. The Id values of τ-H_2Pc were lower than those with α-H_2Pc; moreover, Type I showed higher values than those of Type II. On the contrary, the Iph of Type II showed higher values than those of Type I. As the crystallinity of Type II was promoted by additional milling, the lower conductivity of the τ-form itself is represented. From these results, we can predict that the photoreceptors using Type II for CGL will have better properties, especially for dark decay and photosensitivity, than photoreceptors with Type I CGL.

Electrophotographic Characteristics. Hole carrier drift mobility of the CTL film in this work was shown to be 3.2×10^{-5} $cm^2/V \cdot sec$ at 10^5 V/cm. This mobility is fairly faster compared with mobilities of well-known hydrazone derivatives. Figure 9 and Table I show the typical dark discharge and photo-induced signal discharge curves and the electrophotographic values of the respective H_2Pc/butadiene photoreceptors. The photoresponse of τ-H_2Pc photoreceptors is much higher than that of an α or β-H_2Pc photoreceptor. Additionally, the photoreceptor using Type II exhibited lower dark discharge rate and higher sensitivity than the Type I photoreceptor. These results are consistent with the values of Id and Iph, and with the ratio of Iph/Id from the dark discharge and photocurrent results.

Photosensitivity plots of τ-H_2Pc photoreceptors are shown in Fig. 10. Type II and Type I photoreceptors exhibited at $E_{1/2}$ values of 2.5 ergs/cm^2 and 4.5 ergs/cm^2,

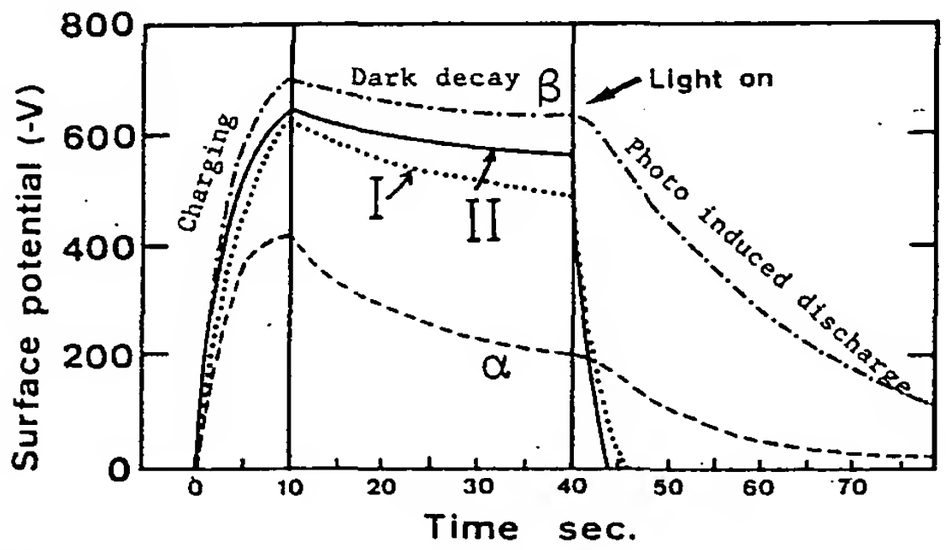

Figure 9. Dark and photo-induced signal discharge curves of H_2Pc photoreceptors.

TABLE I. Electrophotographic Values of H_2Pc Photoreceptors

H_2Pc	Vmax[a] (−V)	DD[b] (V/s)	$E_{1/2}$[c] (lux · sec)	$S_{1/2}$[d] (V/lux · sec)	Vr30[e] (−V)
α	423	7.4	5.99	[f]	24
β	702	2.5	9.13	31	123
τ (Type I)	632	5.1	0.90	181	0
τ (Type II)	651	3.0	0.77	306	0

[a] Vmax = ΔVpid + ΔVdd, where ΔVpid = Vmax/2 − ΔVdd.
[b] DD : Dark decay.
[c] $E_{1/2}$: Half-decay exposure sensitivity.
[d] $S_{1/2}$: $\Delta Vpid/(E_{1/2}) = (Vmax/2 - \Delta Vdd)/(E_{1/2})$.
[e] Vr30 : Residual potential after irradiation (after 30 sec.)
[f] This value cannot be calculated because of a large dark-decay rate.

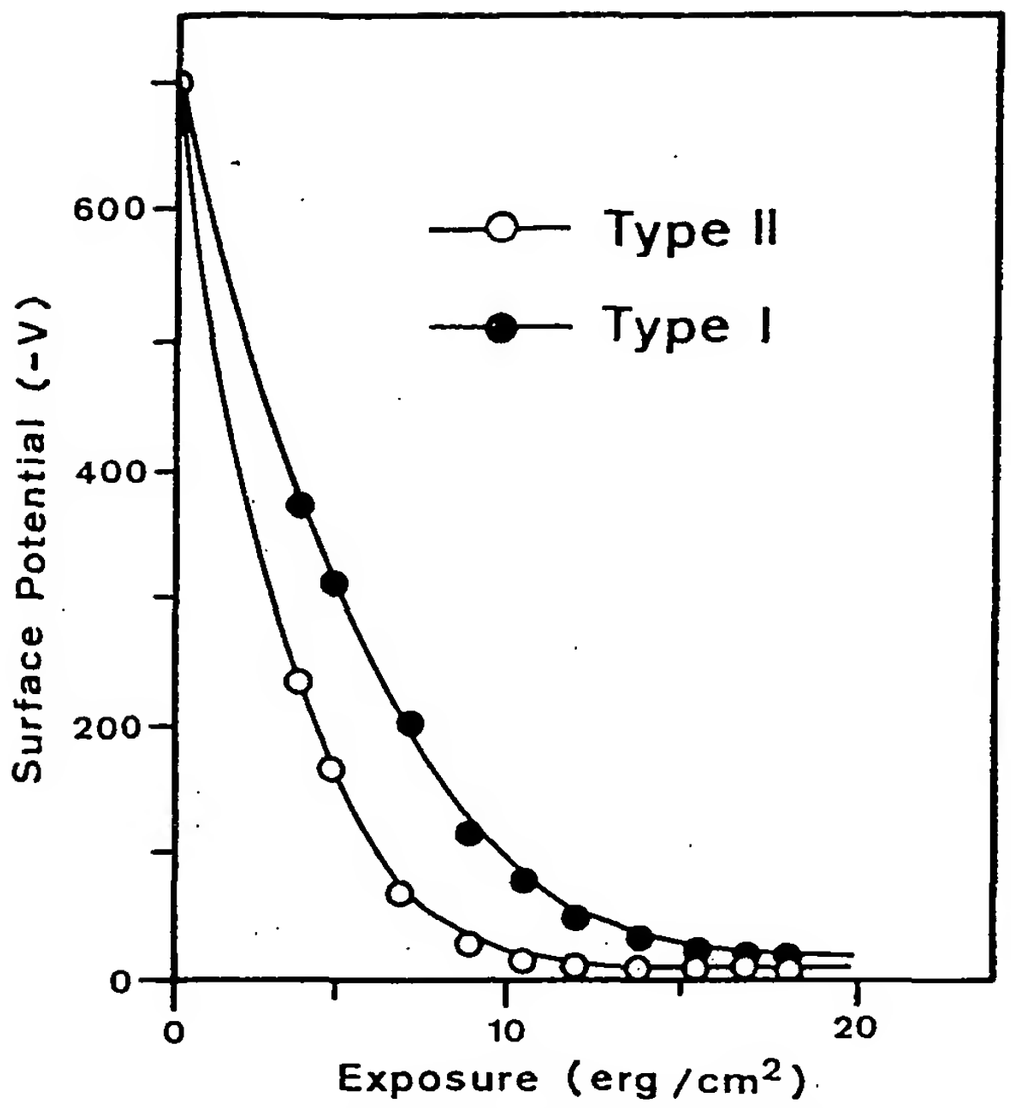

Figure 10. Light discharge curves of H_2Pc photoreceptors.

respectively, at 780 nm, a difference due to the differences of the pigment shapes of the CGM. As the CGL film using granular particles is coated in a plane, it can attain a good injection of holes from CGL to CTL and high hole mobility in the CGL. Figure 11 shows the cyclic plots of Type I and Type II photoreceptors obtained over 1000 cycles using 780-nm light. Both photoreceptors exhibited good cyclic stability.

Summary

We have investigated the characteristics of τ-H_2Pc and the improvement of its particle size as CGM of photoreceptors for LBP applications. As a result of this experiment, the differences of the analytical, electrical, and electrophotographic properties can be seen between needle-like particles (Type I) and granular particles (Type II). The photoreceptor of Type II τ-H_2Pc exhibited much better electrophotographic properties than those of Type I τ-H_2Pc. The half-decay exposure ($E_{1/2}$) of the photoreceptor (CGL = 0.2 μm, CTL = 20 μm) using Type II/butadiene derivative was 2.5 ergs/cm^2 at 780 nm. ⚠

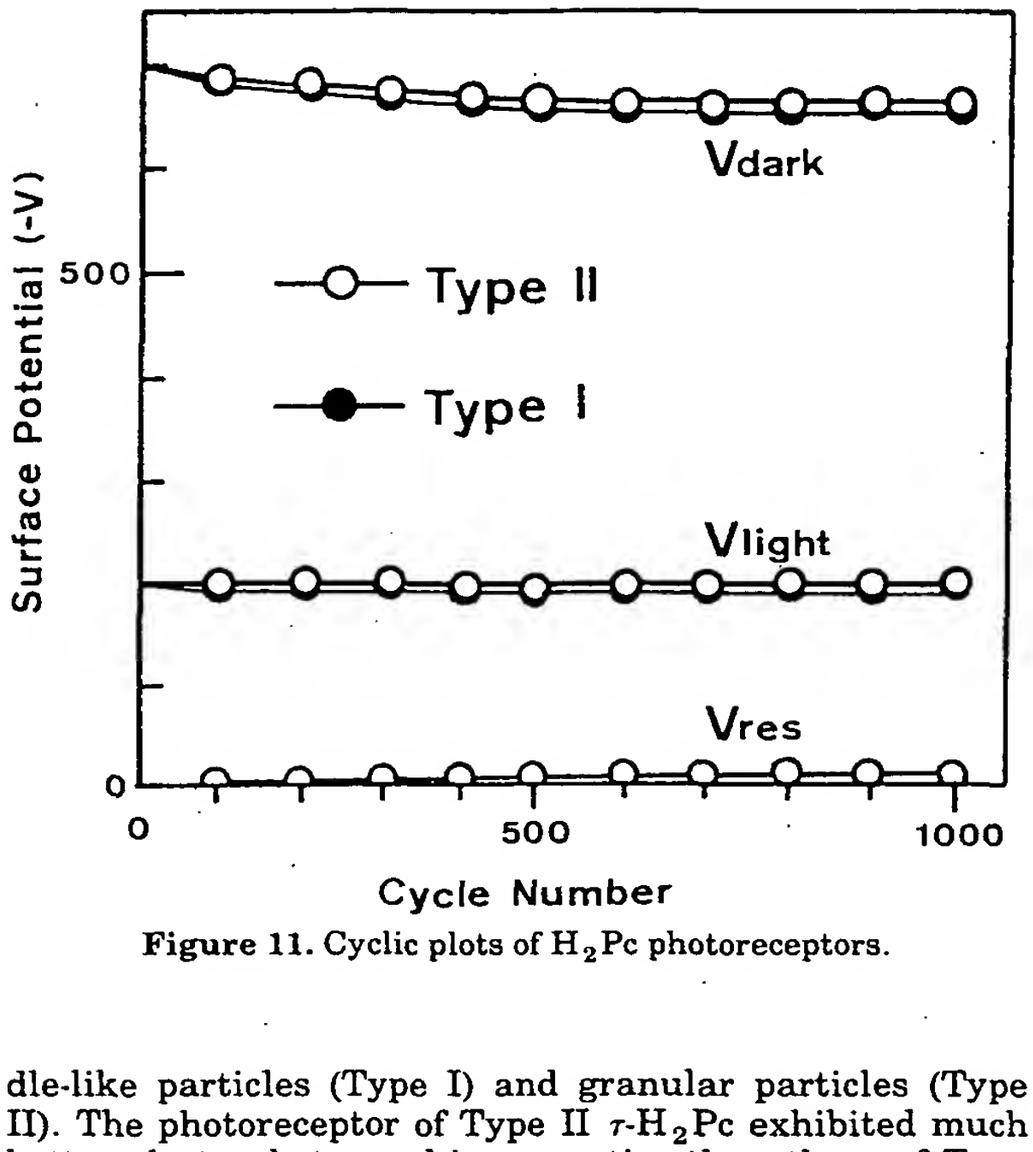

Figure 11. Cyclic plots of H_2Pc photoreceptors.

Acknowledgment. The authors would like to thank Toyo Ink Mfg. Co., Ltd. for its assistance.

References

1. J. H. Sharp and M. Lardon, *J. Phys. Chem.* 72: 3230(1968).
2. S. Takano, T. Enokida, A. Kakuta, and Y. Mori, *Chem. Lett.* 2037(1984).
3. A. Kakuta, Y. Mori, S. Takano, M. Sawada, and I. Shibuya, *J. Imaging. Technol.* 11: 7(1985).
4. J. W. Weigl, J. Mammino, G. L. Whittaker, R. W. Radler, and J. F. Byrne, *Current Problems in Electrophotography*, 1972, p. 287.
5. T. Enokida and R. Hirohashi, *Nippon Kagaku Kaishi* 2: 211(1990).
6. T. Enokida, R. Hirohashi, and N. Morohashi, *Bull. Chem. Soc. Jpn.* 64: 279(1991).
7. B. H. Meier, C. B. Storm, and W. L. Earl, *J. Am. Chem. Soc.* 108: 6074(1986).